

Critical dynamics of phase transition driven by the dichotomous random field

Katsuya Ouchi*

Kobe Design University, 8-1-1 Gakuennishi-Machi, Nishi-ku, Kobe 651-2196, Japan

Takehiko Horita†

Department of Mathematical Informatics,

The University of Tokyo, 7-3-1 Hongo,

Bunkyo-ku, Tokyo 113-8656, Japan

Hirokazu Fujisaka‡

Department of Applied Analysis and Complex Dynamical Systems,

Graduate School of Informatics, Kyoto University, Kyoto 606-8501, Japan

(Dated: December 2, 2024)

Abstract

The time-dependent Ginzburg-Landau equation under the critical temperature driven by a dichotomous stochastic external field with a finite correlation time is studied both numerically and theoretically. The order parameter exhibits two kinds of qualitatively different dynamics, symmetry-restoring motion and symmetry-breaking motion, as the amplitude of the external field is changed. The statistical characteristics discontinuously change at the transition point between the two specific motions, which is quite different from the behavior induced by the system driven by a periodically oscillating field. There exists a region where the order parameter stays for a long time slightly above the transition point, which is referred to as the ‘channel’. The average time of passing through the channels is determined both by using the definition of the probability and by introducing a probabilistic model, which are in agreement with the results of numerical simulation. We further investigate analytically the distribution function of the passage time through the channels and the structure function of the time-series of the order parameter by using the probabilistic model. The results also turn out to be in quite good agreement with those of the numerical simulation.

PACS numbers: 05.40.-a,02.50.-r,05.70.Jk

^{*}Electronic address: ouchi@kobe-du.ac.jp

[†]Present address: Department of Mathematical Science, Osaka Prefecture University, 1-1 Gakuencho, Osaka 599-8531, Japan; Electronic address: horita@ms.osakafu-u.ac.jp

[‡]Electronic address: fujisaka@i.kyoto-u.ac.jp

I. INTRODUCTION

Over the last decade, the dynamics of ferromagnetic systems under critical temperature driven by a periodically oscillating magnetic field have been studied both theoretically [1, 2, 3, 4, 5, 6, 7, 8, 9, 12, 13, 14] and experimentally [10, 11]. It was found that the systems exhibit two qualitatively different characteristic behaviors according to the frequency Ω and the amplitude h of the applied magnetic field. For small frequency Ω with h exceeding the critical value h_c , the magnetization oscillates so as to restore the symmetry of the system because individual spins constituting the ferromagnet can follow the slow variation of the field, and such oscillation is referred to as symmetry-restoring oscillation (SRO). On the other hand, the spins cannot follow the field at sufficiently high frequencies Ω , and then we observe the magnetization oscillation without symmetry, which is referred to as symmetry-breaking oscillation (SBO). It has furthermore been established that there exists a transition point Ω_c between SRO and SBO characterized as a kind of the second-order phase transition, which is referred to as the dynamical phase transition (DPT). In fact, it was reported that the amplitude of SBO increases in the power law form [4] for deviation from the transition point.

The DPT was first observed numerically in the deterministic mean-field system for a ferromagnet in an oscillating field [1, 2], and has subsequently been studied in numerous Monte Carlo simulations of the kinetic Ising system under critical temperature [3, 4, 5, 6, 7, 8, 9]. It has also been observed experimentally in ultra-thin Co films on Cu(100) [10, 11].

In recent years, Fujisaka et al. have investigated the DPT by introducing a simple model equation, i.e., the time-dependent Ginzburg-Landau equation in an external field [12],

$$\frac{ds(\mathbf{r}, t)}{dt} = (T_c - T)s - s^3 + D\nabla^2 s + F(t), \quad (T < T_c) \quad (1)$$

where T is the temperature of the system, T_c is the critical temperature, D is a diffusion constant and $F(t)$ is an oscillating external field expressed as, e.g., $F(t) = h \cos(\Omega t)$ with an amplitude h and a frequency Ω . $s(\mathbf{r}, t)$ expresses an order parameter of the system, which depends, in general, on not only the time t but also the position \mathbf{r} . In considering the ferromagnetic system, Eq. (1) physically represents the dynamics of the local magnetization $s(\mathbf{r}, t)$ of an Ising-type ferromagnet under the critical temperature T_c driven by the temporally oscillating magnetic field $F(t)$ applied along the easy axis of the ferromagnet.

Equation (1) can be reduced to a simpler form

$$\frac{ds(t)}{dt} = (T_c - T)s - s^3 + F(t), \quad (2)$$

provided that spatial fluctuations can be neglected, i.e., the order parameter is independent of the position \mathbf{r} .

The SBO and SRO are easily demonstrated numerically by using Eq. (2) and the transition point between the two distinct oscillations is determined analytically by applying the Floquet analysis and the Fourier expansion method, which gives the phase diagram in the (h, Ω) plane [12, 14]. Fujisaka et al. have further revealed that the DPT belongs to the same universality class as the second-order phase transition in the equilibrium critical phenomena [12]. They have also investigated several other systems in the oscillating external field, for example, isotropic or anisotropic X-Y spin system [13, 14], tristable spin system [14], and so on, where a greater variety of DPTs are observed.

The authors of Refs. [12, 14] focused on the discussion on the DPT driven by the oscillating external field. It is quite interesting to ask whether the DPT is universally shown in driving by different kinds of external fields, e.g., randomly modulating field. If one provides a random external field with a correlation time τ_f , then the field may be regarded as a kind of oscillating field with an average frequency $2\pi/\tau_f$, and then a similar analysis on the possibility of existence of the symmetry-breaking transition may be developed.

In the present paper, we investigate the dynamics subject to Eq. (2) driven by a dichotomous stochastic external field (DSEF) $F(t)$ as an example of the random external field, where $F(t)$ takes only two values, i.e., either $+H_0$ or $-H_0$ with a constant $H_0 > 0$. We use such a field because it is obviously expected that random fields with unlimited amplitude, e.g., the Gaussian colored noise, cause no distinct transition. The DSEF is one of the simplest discrete Markovian processes with a finite correlation time and a confined amplitude, and is not only easily investigated in numerical and theoretical analysis but can also be generated in laboratory experiments.

It is obvious that $s(t)$ yields a stochastic motion around $\langle s(t) \rangle \neq 0$ in a sufficiently weak DSEF case, which is referred to as the symmetry breaking motion (SBM) by analogy with the DPT. On the other hand, $s(t)$ will yield a stochastic motion around $\langle s(t) \rangle = 0$ in a sufficiently strong DSEF case, which is referred to as the symmetry restoring motion (SRM). We will show the existence of the transition point separating SBM and SRM as

the intensity of the DSEF is increased, and discuss several statistical characteristics in the vicinity of the transition point and reveal similarities and differences between the dynamics in the oscillating field case and those in the present DSEF case.

The present paper is constructed as follows. In Sec. II, the equation of motion studied in this paper is introduced and the definition and several properties of the DSEF are summarized. In Sec. III, we discuss the dynamics of the SBM and the stationary probability distribution function of the magnetization in an analytical way. In Sec. IV, we then discuss the dynamics of the SRM and the stationary distribution of the magnetization, where it will turn out that the behavior drastically changes at the transition point between SBM and SRM. In Sec. V, the process of the magnetization passing through channels, which are defined in the text, is investigated and the average time of the process is obtained. In Sec. VI, a probabilistic model simplifying the dynamics of passing through a channel in the SRM phase is introduced and several statistical characteristics are analytically developed. The results are individually compared with numerical simulations. Concluding remarks are given in Sec. VII.

II. MODEL EQUATION DRIVEN BY THE DSEF

We consider the time-dependent Ginzburg-Landau equation driven by the DSEF $F(t)$,

$$\frac{ds(t)}{dt} = s - s^3 + F(t). \quad (3)$$

This equation is obtained after the rescaling $t \rightarrow (T_c - T)^{-1}t$, $s \rightarrow (T_c - T)^{1/2}s$ and $H_0 \rightarrow (T_c - T)^{3/2}H_0$ in Eq. (2).

We first summarize the definition, notations, and several properties of $F(t)$. The DSEF $F(t)$ continues to take an identical value $+H_0$ ($-H_0$) longer than time τ with the probability $p(\tau)$ and then jumps to another value $-H_0$ ($+H_0$), where $p(\tau)$ is given, in terms of $t = -\tau_f \ln r$ with an uniformly distributed number r between 0 and 1, as

$$p(\tau) \equiv Pr[t > \tau] = Pr[r < e^{-\tau/\tau_f}] = e^{-\tau/\tau_f} \quad (4)$$

with τ_f being proportional to the correlation time. In fact, the autocorrelation function of the applied field is evaluated as

$$\langle F(\tau)F(0) \rangle = H_0^2 e^{-2\tau/\tau_f}, \quad (5)$$

where $\langle \cdots \rangle$ is the ensemble average. The probability density $\rho(\tau)$ that $F(t)$ continues to take $+H_0$ ($-H_0$) during τ and then jumps to $-H_0$ ($+H_0$) is given, in terms of $p(\tau)$, by

$$p(\tau) = \int_{\tau}^{\infty} \rho(s) ds. \quad (6)$$

Equation (6) reads

$$\rho(\tau) = \tau_f^{-1} e^{-\tau/\tau_f}. \quad (7)$$

If the DSEF is not applied to the system, then $s(t)$ subject to Eq. (3) with $H_0 = 0$ eventually approaches either of the stationary fixed points ± 1 , one of which is selected by the sign of the initial condition $s(0)$. In applying the DSEF, the motion of $s(t)$ is confined in the range of either $s(t) > 0$ or $s(t) < 0$ for any τ_f provided that the amplitude H_0 of the DSEF is below the critical value

$$H_c \equiv 2(1/3)^{3/2} = 0.3849 \dots \quad (8)$$

One of the ranges is selected according to the initial condition. On the other hand, it will be shown in Sec. III that the motion of $s(t)$ for $H_0 > H_c$ is expanded discontinuously in the range of $-s_+ < s(t) < s_+$ with a constant s_+ which is independent of τ_f . So the qualitative behavior in Eq. (3) is distinguished only by whether $H_0 < H_c$ or $H_0 > H_c$, where the result does not depend on τ_f . We then discuss each characteristic of the dynamics for $H_0 < H_c$ and for $H_0 > H_c$.

III. DYNAMICS AND STATISTICAL CHARACTERISTICS IN THE SBM PHASE ($H_0 < H_c$)

Let us first consider the dynamics of the equations

$$\dot{s} = s - s^3 + \epsilon H_0, \quad (\epsilon = \pm 1) \quad (9)$$

i.e., the external field $F(t)$ is not the DSEF but fixed to a constant $+H_0$ or $-H_0$. Equation (9) for $H_0 < H_c$ is analytically integrated in the form

$$t = -\ln \left(\left| \frac{s(t) - s_{1\pm}}{s_0 - s_{1\pm}} \right|^{\alpha_{1\pm}} \left| \frac{s_0 - s_{2\pm}}{s(t) - s_{2\pm}} \right|^{\alpha_{2\pm}} \left| \frac{s(t) - s_{3\pm}}{s_0 - s_{3\pm}} \right|^{\alpha_{3\pm}} \right), \quad (10)$$

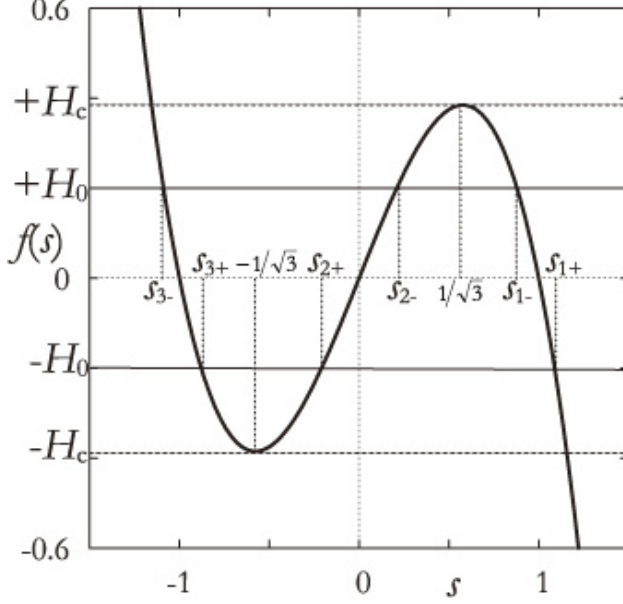


FIG. 1: Positions of $s_{j\pm}$ for $j = 1, 2$, and 3 . Individual s_{j+} and s_{j-} correspond to the solutions of the algebraic equations $s - s^3 + H_0 = 0$ and $s - s^3 - H_0 = 0$ for $H_0 < H_c$, respectively. The value of H_c is simultaneously exhibited in a schematic way.

where $s_0 = s(0)$ and $s_{1\pm}$, $s_{2\pm}$, and $s_{3\pm}$ are all the solutions of the algebraic equations

$$s - s^3 + \epsilon H_0 = 0. \quad (11)$$

The positions of $s_{j\pm}$ for $j = 1, 2$, and 3 are schematically exhibited in Fig. 1 and the explicit forms are given by

$$s_{1\pm} = \cos \varphi \pm \frac{1}{\sqrt{3}} \sin \varphi, \quad (12)$$

$$s_{2\pm} = \mp \frac{2}{\sqrt{3}} \sin \varphi, \quad (13)$$

$$s_{3\pm} = - \left(\cos \varphi \mp \frac{1}{\sqrt{3}} \sin \varphi \right), \quad (s_{3\pm} = -s_{1\mp}) \quad (14)$$

respectively, where φ is determined as $\sin(3\varphi) = H_0/H_c$. The exponents $\alpha_{j\pm}$ ($j = 1, 2, 3$) in Eq. (10) are given by

$$1/\alpha_{1\pm} = (s_{1\pm} - s_{2\pm})(s_{1\pm} - s_{3\pm}) = 1 + 2 \sin \left(\frac{\pi}{6} \pm 2\varphi \right) \quad (15)$$

$$1/\alpha_{2\pm} = (s_{1\pm} - s_{2\pm})(s_{2\pm} - s_{3\pm}) = -1 + 2 \cos 2\varphi \quad (16)$$

$$1/\alpha_{3\pm} = (s_{1\pm} - s_{3\pm})(s_{2\pm} - s_{3\pm}) = 1 + 2 \sin \left(\frac{\pi}{6} \mp 2\varphi \right), \quad (17)$$

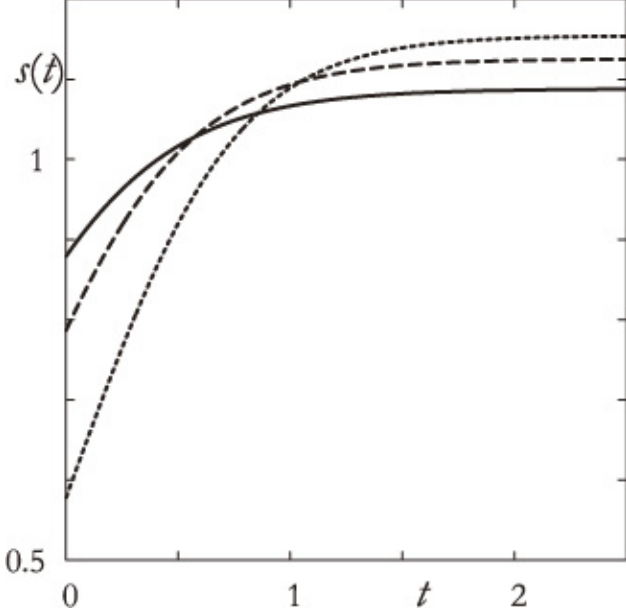


FIG. 2: Three temporal evolutions of the order parameter $s(t)$ subject to Eq. (9) with $+H_0$ ($H_0 < H_c$), which is analytically integrated in the form Eq. (10). The magnitude H_0 is set to be $H_0 = 0.2$ (line), 0.3 (dashed line), and 0.3849 (dotted line), respectively, where all the initial conditions are set to be $s_0 = s_{1-}$. It is shown that all the orbits monotonously approach individual s_+ determined by Eq. (12) as time elapses.

respectively, where $\alpha_{1\pm} = \alpha_{3\mp}$ and $\alpha_{2+} = \alpha_{2-}$ hold. Figure 2 shows several orbits evaluated from Eq. (10) for $s_0 = s_{1-}$ and $F(t) = +H_0$, which shows that each $s(t)$ monotonously approaches s_{1+} as time goes on. On the other hand, all the orbits approach s_{1-} when $F(t)$ jumps to $-H_0$, and so the orbits are all confined in the range $s_{1-} < s(t) < s_{1+}$ in considering the case of $F(t)$ being the DSEF. It is obvious that there exist other orbits which are confined in the range $s_{3-} < s(t) < s_{3+}$. Indeed, these two kinds of orbits are the examples of the SBM denoted above.

There also exists an unstable SRM $s_u(t)$ confined in the range $s_{2+} < s_u(t) < s_{2-}$. For a given sample of time series $F(t)$, $s_u(t)$ is uniquely determined corresponding to the explicit form of $F(t)$. The SBM confined in the range $s_{1-} < s(t) < s_{1+}$ emerges provided that the initial point $s(t_0)$ at a time t_0 satisfies the condition $s(t_0) > s_u(t_0)$. Otherwise, the SBM confined in the range $s_{3-} < s(t) < s_{3+}$ emerges. Two SBMs and an unstable SRM are shown in Fig. 3 which is obtained by numerically integrating Eq. (3). One finds that the unstable SRM is located between the two SBMs and that none of the motions overlap. Throughout

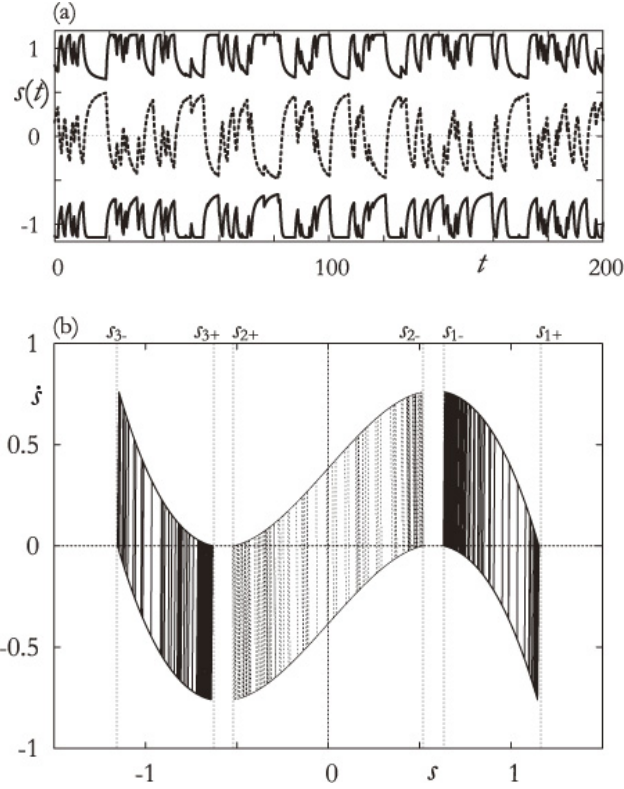


FIG. 3: (a) Time dependence and (b) the motion on the (s, \dot{s}) plane of two SBMs (solid lines) and one unstable SRM (dashed line) are drawn. The two SBMs are evaluated by numerically integrating Eq. (3) for $H_0 = 0.38$ and $\tau_f = 5$. The unstable SRM is then numerically evaluated by replacing $t \rightarrow -t$ in Eq. (3) for the same control parameters, where the motion is found to be a stable one.

this paper, the numerical integration of Eq. (3) is carried out by using the Euler difference scheme with the time increment $\Delta t = 1/100$. The dichotomous external field $F(t)$ in Eq. (3) is numerically generated according to the definition of Eq. (4).

Let us present the stationary distribution function of the SBM to discuss quantitatively the stochastic process. In considering a general nonlinear Langevin equation of motion driven by the dichotomous force $F(t)$,

$$\dot{x}(t) = f(x) + g(x)F(t) \quad (18)$$

where $f(x)$ and $g(x)$ are generally nonlinear functions of x , the temporal evolution of the

distribution function $P(x, F, t)$ for the pair process $[x(t), F(t)]$ is determined by [15, 17, 18]

$$\begin{aligned}\frac{\partial}{\partial t}P(x, t) &= -\frac{\partial}{\partial x}[f(x)P(x, t) + H_0g(x)q(x, t)], \\ \frac{\partial}{\partial t}q(x, t) &= -\frac{2}{\tau_f}q(x, t) - \frac{\partial}{\partial x}[f(x)q(x, t) + H_0g(x)P(x, t)],\end{aligned}\quad (19)$$

where $P(x, t) \equiv P(x, +H_0, t) + P(x, -H_0, t)$ and $q(x, t) \equiv P(x, +H_0, t) - P(x, -H_0, t)$ are introduced. The stationary distribution $P^{st}(x) \equiv P(x, \infty)$ in Eq. (19) is solved in the form

$$P^{st}(x) = N \frac{g(x)}{H_0^2 g(x)^2 - f(x)^2} \exp \left\{ -\frac{1}{\tau_f} \int^x dx' \left[\frac{1}{f(x') - H_0 g(x')} + \frac{1}{f(x') + H_0 g(x')} \right] \right\} \quad (20)$$

with a normalization constant N , provided that each equation

$$\dot{x} = f(x) + H_0 g(x), \quad \dot{x} = f(x) - H_0 g(x) \quad (21)$$

has a finite steady and stable solution.

In the case of Eq. (3), substituting $f(x) = x - x^3$ and $g(x) = 1$ into Eq. (20) implies that the stationary distribution function $P_{SBM}^{st}(s)$ in the SBM ($H_0 < H_c$) is written as

$$P_{SBM}^{st}(s) \propto |s^2 - s_{1+}^2|^{-\beta_{1+}} |s^2 - s_{1-}^2|^{-\beta_{1-}} |s^2 - s_{2+}^2|^{-\beta_{2+}} \quad (22)$$

where $\beta_{k\pm} = 1 - 1/(\tau_f \alpha_{k\pm})$ with $k = 1$ and 2. The exact analytic form of Eq. (22) is confirmed by comparing to the numerically evaluated distribution function for $H_0 = 0.3$ and $\tau_f = 5$ in Fig. 4. It should be noted that Eqs. (22) and (14) reveal that the confined region of $s(t)$ is independent of τ_f .

IV. DYNAMICS AND STATISTICAL CHARACTERISTICS IN THE SRM PHASE ($H_0 > H_c$)

Next we consider the dynamics of Eq. (9) for $H_0 > H_c$. Equation (9) for $H_0 > H_c$ is integrated analytically in the form

$$\begin{aligned}t &= -\frac{1}{2(3s_{\pm}^2 - 1)} \ln \frac{(s - s_{\pm})^2}{s^2 + s_{\pm}s + s_{\pm}^2 - 1} \frac{s_0^2 + s_{\pm}s_0 + s_{\pm}^2 - 1}{(s_0 - s_{\pm})^2} \\ &\quad + \frac{6s_{\pm}}{2(3s_{\pm}^2 - 1)\sqrt{3s_{\pm}^2 - 4}} \left[\arctan \left(\frac{2s + s_{\pm}}{\sqrt{3s_{\pm}^2 - 4}} \right) - \arctan \left(\frac{2s_0 + s_{\pm}}{\sqrt{3s_{\pm}^2 - 4}} \right) \right],\end{aligned}\quad (23)$$

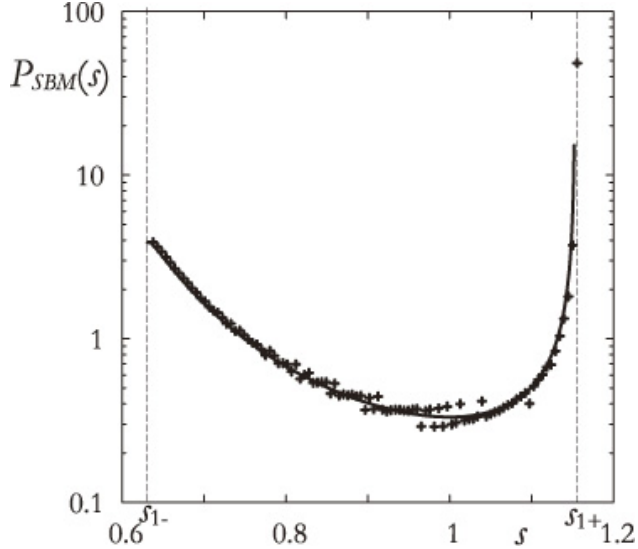


FIG. 4: Stationary distribution function obtained both analytically (solid line) and numerically (symbols), where only the distribution in the range $s_{1-} < s(t) < s_{1+}$ is drawn. The control parameters are set to be $H_0 = 0.3$ and $\tau_f = 5$. It should be noted that the analytical result is in good agreement with that of the numerical simulation.

where $s_0 = s(0)$ and s_{\pm} are the solutions of Eq. (11) which are expressed in the form

$$s_{\pm} = \left[\frac{1}{2} \left(\pm H_0 + \sqrt{H_0^2 - H_c^2} \right) \right]^{1/3} + \left[\frac{1}{2} \left(\pm H_0 - \sqrt{H_0^2 - H_c^2} \right) \right]^{1/3}, \quad (24)$$

where $s_+ = -s_-$ holds. The positions of s_{\pm} are schematically exhibited in Fig. 5. Figure 6 shows several orbits evaluated from Eq. (23) with $s_0 = s_-$ and $F(t) = +H_0$, which means that $s(t)$ approaches s_+ in the limit $t \rightarrow \infty$. It further indicates that $s(t)$ stays for a long time in the vicinity of $s = -1/\sqrt{3}$ for H_0 slightly above H_c , which is referred to as the ‘channel’ and is schematically exhibited in Fig. 5. On the other hand, all the orbits approach s_- when $F(t)$ jumps to $-H_0$, where the channel is located at $s = 1/\sqrt{3}$. The position of the channel is denoted by s_{ch} , where $s_{ch} \equiv \mp 1/\sqrt{3}$ for $F(t) = \pm H_0$.

If H_0 is far from H_c , then $s(t)$ easily passes through the channels and the orbit will be confined in the range $s_- < s(t) < s_+$, which is the SRM mentioned above. An orbit in the SRM phase for $H_0 = 0.5$ and $\tau_f = 10$ is shown in Fig. 7. The comparison between Figs. 3 and 7 exhibits that the SRM for $H_0 > H_c$ is constructed via an ‘attractor merging crisis’ of two SBMs and one unstable SRM coexisting for $H_0 < H_c$. The fact that $s_{j\pm}$ with $j = 1, 2$, and 3 determining the boundaries of the two SBMs and one unstable SRM are all dependent

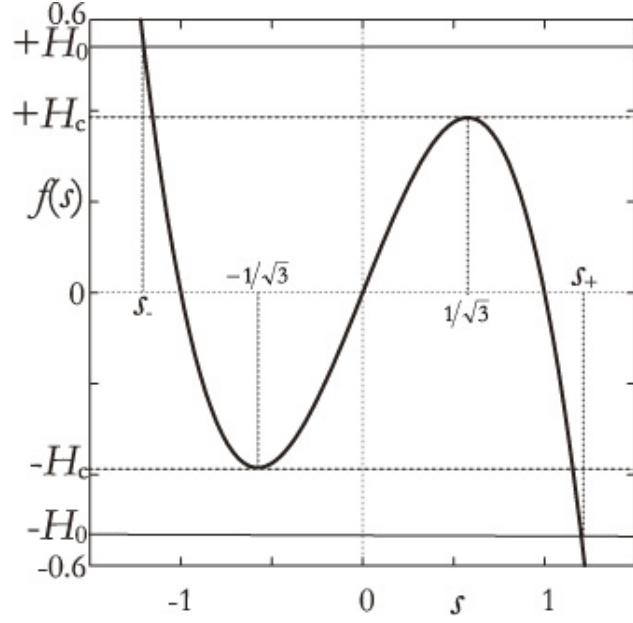


FIG. 5: Positions of s_{\pm} . s_+ and s_- are the solutions of the algebraic equations $s - s^3 + H_0 = 0$ and $s - s^3 - H_0 = 0$ for $H_0 > H_c$, respectively. The positions of channels $s = \pm 1/\sqrt{3}$ are also indicated in this figure.

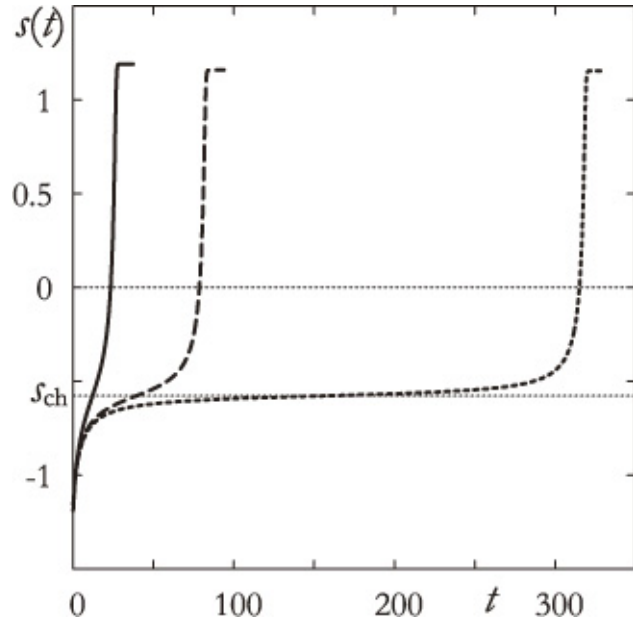


FIG. 6: Three orbits subject to Eq. (9) with $+H_0$ for $H_0 > H_c$, which is analytically integrated in the form Eq. (23). The magnitude H_0 is set to be $H_0 = 0.386$ (dotted line), 0.4 (dashed line), and 0.5 (solid line), respectively, where all the initial conditions are set to be $s_0 = s_-$.

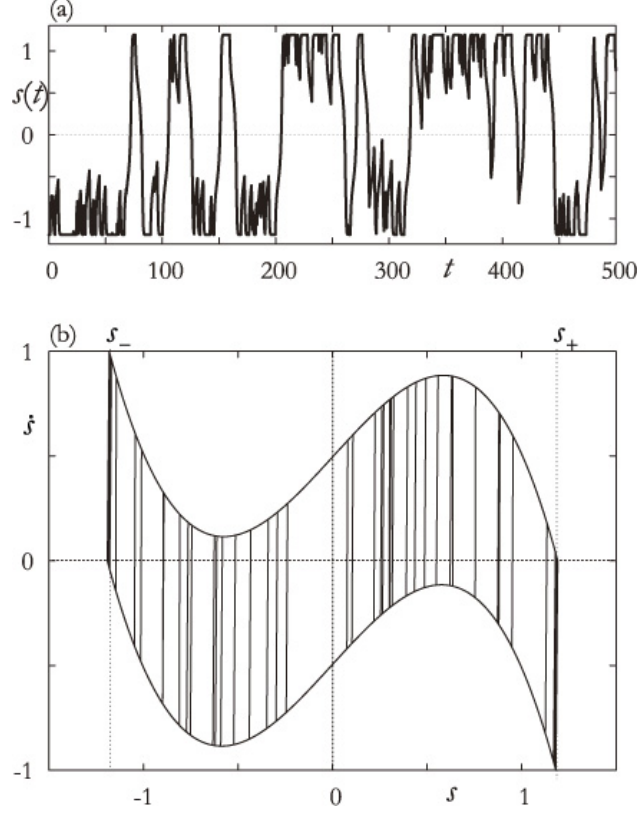


FIG. 7: (a) Time dependence and (b) the motion on the (s, \dot{s}) plane of a SRM are drawn. The orbit is evaluated by numerically integrating Eq. (3) for $H_0 = 0.5$ and $\tau_f = 10$.

only on H_0 suggests that the transition point between SBM and SRM is determined only as $H_0 = H_c$.

Let us find the stationary distribution function of the SRM to characterize the stochastic process and to discuss whether or not $s(t)$ passes through the channels for $H_0 > H_c$. One can analytically solve Eq. (20) for $H_0 > H_c$ which yields the stationary distribution function $P_{SRM}^{st}(s)$ of the SRM in the form

$$\begin{aligned}
 P_{SRM}^{st}(s) \propto & |s^2 - s_+^2|^{-\frac{\tau_f^{-1}}{3s_+^2-1}-1} [(s^2 + s_+^2 - 1)^2 - s_+^2 s^2]^{-\frac{\tau_f^{-1}}{3s_+^2-1}-1} \\
 & \times \exp \left\{ \frac{\tau_f^{-1} s_+}{(s_+^2 - 1/3) \sqrt{3s_+^2 - 4}} \left[\arctan \left(\frac{2s - s_+}{\sqrt{3s_+^2 - 4}} \right) \right. \right. \\
 & \left. \left. - \arctan \left(\frac{2s + s_+}{\sqrt{3s_+^2 - 4}} \right) \right] \right\}. \tag{25}
 \end{aligned}$$

The analytic form (25) is confirmed by comparing to the numerically evaluated distribution function for $H_0 = 0.39, 0.4$, and 0.5 by keeping $\tau_f = 10$ in Fig. 8, which shows that $s(t)$

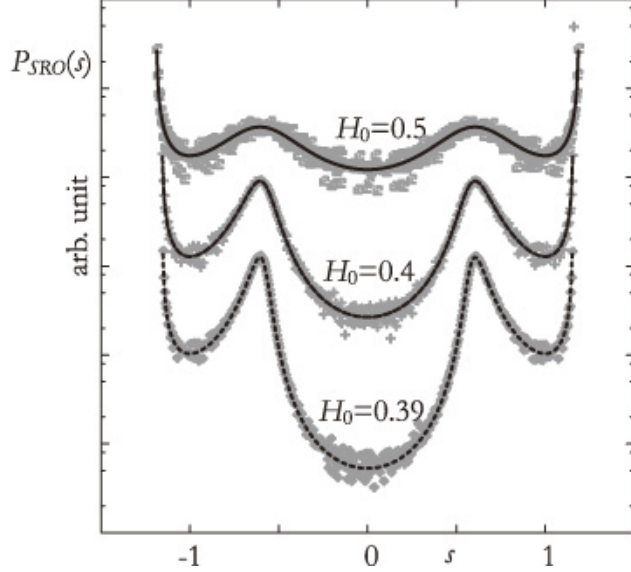


FIG. 8: Stationary probability distribution functions obtained both analytically (lines) and numerically (symbols) for three values of H_0 by keeping $\tau_f = 10$. It should be noted that the analytical and simulational results for each H_0 are normalized so as to align with each other.

certainly passes through s_{ch} because $P_{SRM}^{eq}(s)$ for $s > 0$ is connected with that for $s < 0$. It turns out that the form of the stationary probability distribution function is changed drastically from Eq. (25) to Eq. (22) at $H_0 = H_c$. This phenomenon is generally known as the noise induced phase transition [16, 17, 18]. As the result, the transition line between SRM and SBM is determined by $H_0 = H_c$ and is independent of τ_f . The phase diagram is shown in Fig. 9. Furthermore, the ensemble average of $s(t)$, $\langle s(t) \rangle$, depends discontinuously on H_0 at $H_0 = H_c$ as shown in Fig. 10. This behavior is quite different from that of the system driven by periodically oscillating field such as $F(t) = h \cos(\Omega t)$ [4, 12], where the transition line between SRM and SBM depends not only on the amplitude h but also on the frequency Ω , and $\langle s(t) \rangle$ is characterized as a second-order phase transition, i.e., continuous transition with respect to the control parameter.

V. AVERAGE TIME OF PASSING THROUGH THE CHANNELS s_{ch}

Equation (25) suggests that the probability of passing through s_{ch} is quite small for $0 < H_0 - H_c \ll 1$. In fact, the probability $P_{SRM}^{st}(0)$ in Eq. (25), which estimates how the

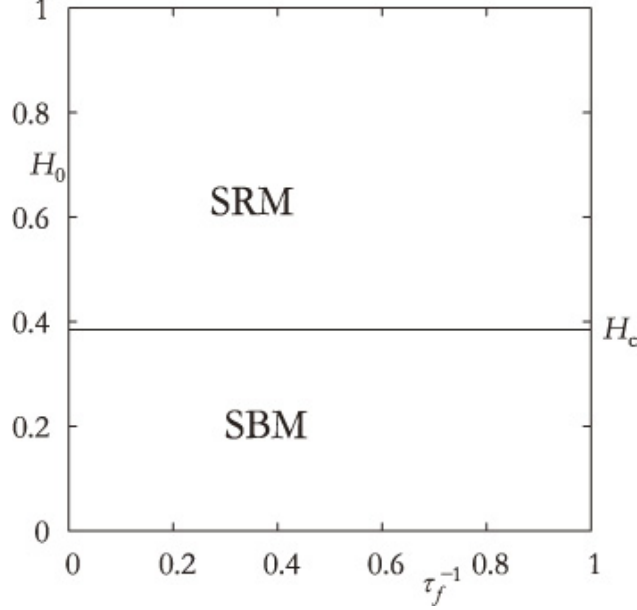


FIG. 9: Phase diagram on the (τ_f^{-1}, H_0) plane where the transition line separating the SRM and SBM is drawn. Transition line is independent of τ_f^{-1} and is simply given as $H_0 = H_c$.

passage probability depends on H_0 and τ_f , is evaluated as

$$P_{SRM}^{st}(0) \propto \exp \left[-\frac{\pi}{3^{5/4}} \tau_f^{-1} (H_0 - H_c)^{-1/2} \right]. \quad (26)$$

Figure 11 shows numerically obtained temporal evolutions of $s(t)$ for $H_0 = 0.388$ and 0.385 , which appears to indicate that the time of passing through s_{ch} increases as H_0 approaches H_c . Let us estimate analytically the average time $\bar{\tau}$ of passing through s_{ch} .

The minimal passage time denoted as τ_{ch} is estimated by integrating Eq. (9) around $s \simeq s_{ch}$. By setting $u(t) = s(t) - s_{ch}$ and assuming $u \ll s_{ch}$, Eq. (9) with $\epsilon = -1$ is approximated to the form

$$\dot{u} = -3s_{ch}u^2 - (H_0 - H_c), \quad (27)$$

which is straightforwardly integrated to give

$$u(t) = -\sqrt{\frac{H_0 - H_c}{3s_{ch}}} \tan \left[\sqrt{3s_{ch}(H_0 - H_c)} t \right] \quad (28)$$

with the initial condition $u(0) = 0$. Equation (28) reads

$$\tau_{ch} = \frac{C}{(H_0 - H_c)^{1/2}}, \quad C = \frac{\pi}{2\sqrt{3s_{ch}}}. \quad (29)$$

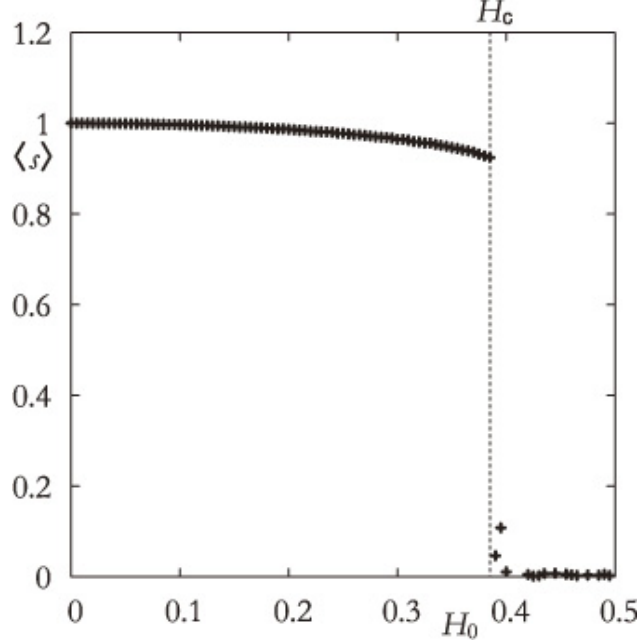


FIG. 10: $\langle s \rangle$ vs H_0 for $\tau_f = 5$. One finds that $\langle s \rangle$ is disconnected at $H_0 = H_c$.

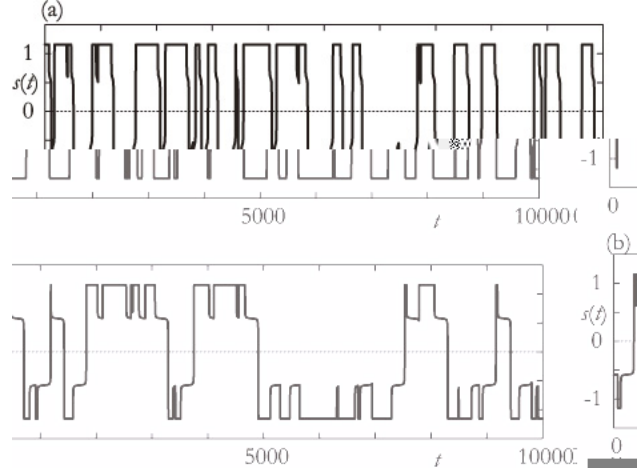


FIG. 11: Time series of $s(t)$ for (a) $H_0 = 0.388$ and (b) 0.385 by keeping $\tau_f = 200$.

In considering the process of passing through s_{ch} when the system is driven by the DSEF $F(t)$, the condition for passing through s_{ch} is that $F(t)$ continues to take an identical value longer than τ_{ch} . When H_0 and τ_f are set for the two time scales τ_f and τ_{ch} to satisfy $\tau_f > \tau_{ch}$, Eq. (4) implies that $p(\tau_{ch}) = e^{-\tau_{ch}/\tau_f} \simeq 1$, i.e., that $F(t)$ frequently satisfies the condition for passing through s_{ch} . Therefore, $\bar{\tau}$ for $\tau_f > \tau_{ch}$ is nearly equivalent to τ_{ch} ,

$$\bar{\tau} \simeq \tau_{ch} = \frac{C}{(H_0 - H_c)^{1/2}}, \quad (30)$$

which is identical to the result of the Landau theory in the second-order phase transition phenomena.

In the case of $\tau_f \ll \tau_{ch}$, on the other hand, Eq. (4) gives $p(\tau_{ch}) \ll 1$, which implies that the probability of $F(t)$ continuing to take the identical value longer than τ_{ch} is much smaller and therefore that $\bar{\tau}$ is much longer than τ_{ch} because it needs a long time to satisfy the condition for passing through s_{ch} .

$\bar{\tau}$ for $\tau_f \ll \tau_{ch}$ is explicitly determined as follows. For a long $\bar{\tau}$, let us divide $\bar{\tau}$ into subintervals each of which is the time τ_f . The individual divided time series are regarded to be approximately independent of each other because τ_f is the same order as the correlation time of $F(t)$. Therefore, $\tau_f/\bar{\tau}$ is the probability that $s(t)$ passes through s_{ch} once because $\bar{\tau}$ is the average time of passing through s_{ch} . On the other hand, $p(\tau_{ch})$ is the probability for $s(t)$ to pass through s_{ch} once by the definition of the probability. The above two results give the relation $p(\tau_{ch}) \simeq \tau_f/\bar{\tau}$, which directly leads to

$$\bar{\tau}^{-1} \simeq \tau_f^{-1} e^{-\tau_{ch}/\tau_f} = \tau_f^{-1} \exp \left[-\frac{C}{\tau_f (H_0 - H_c)^{1/2}} \right] \quad (31)$$

with the constant C defined in Eq. (29). Equation (31) reveals that the average time of passing through the channel s_{ch} depends on $H_0 - H_c$ in a stretched exponential form for $\tau_f \ll \tau_{ch}$. The dependence of $\bar{\tau}$ on $H_0 - H_c$ is confirmed by comparing with the numerical simulation in Fig. 12. One should note that the form (31) is same as that for the result of chaotic phase synchronization in coupled chaotic oscillators [19, 20, 21, 22, 23, 24, 25].

VI. PROBABILISTIC MODEL

In order to discuss the statistical characteristics of the dynamics passing through the channels for $\tau_f \ll \tau_{ch}$, we here propose a probabilistic model. The behaviors of $s(t)$ we attempt to model are first summarized. The initial condition of $s(t)$ is set to be in the vicinity of s_+ . If a time interval of $F(t)$ satisfying the condition $F(t) = -H_0$ becomes longer than τ_{ch} for the first time, then $s(t)$ passes through s_{ch} and approaches s_- in the time interval. See Fig. 13. The event in which $s(t)$ jumps from s_+ to s_- occurs only in this case. It should be noted that the jumps from $s(t) > 0$ ($s(t) < 0$) to $s(t) < 0$ ($s(t) > 0$) are approximately independent of subsequent jumps.

Let us discretize the time t in the form $t = k\Delta t$, ($k = 1, 2, 3, \dots$) as a simple approach to

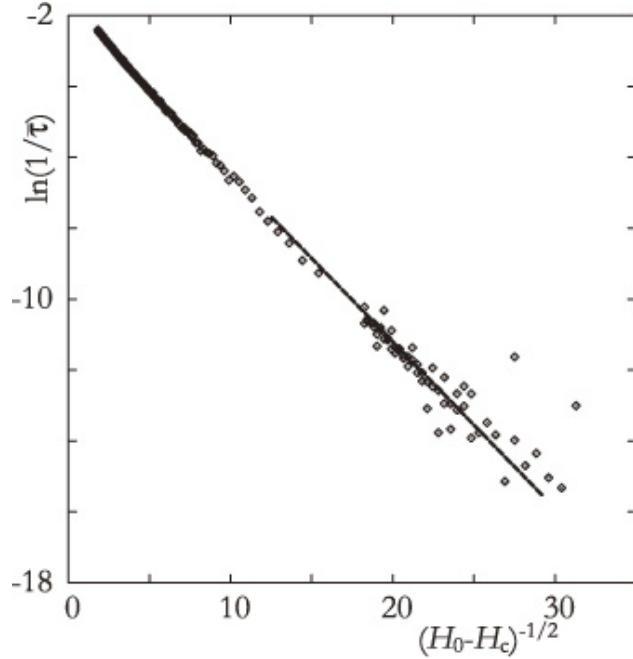


FIG. 12: The dependence of $\bar{\tau}$ on $H_0 - H_c$ determined numerically for $\tau_f = 5$. $\bar{\tau}$ for a given H_0 is obtained by integrating Eq. (3) until a time T and simultaneously by counting the number N of times passing through the position $s = 0$, where $\bar{\tau}$ is evaluated as $\bar{\tau} = T/N$. One finds that $\ln \bar{\tau}^{-1}$ linearly depends on $(H_0 - H_c)^{-1/2}$ in the region of $0 < H_0 - H_c \ll 1$, where the dashed line is expressed as $\ln y = Ax + B$ with fitting coefficients A and B .

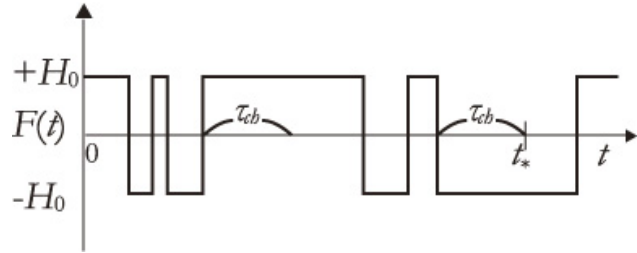


FIG. 13: The time that $s(t)$ jumps from s_+ to s_- is indicated schematically in the time series of $F(t)$. $s(t)$ jumps at the time t_* in this case, where $F(t)$ takes the value $-H_0$ longer than τ_{ch} for the first time in the time series of $F(t)$.

construct the probabilistic model according to the process noted above, where Δt is a certain small time step. Then, τ_{ch} is discretized as $\tau_{ch} \equiv n_{ch}\Delta t$ with the corresponding integer n_{ch} . $F(t)$ is assumed to keep the value for the interval of Δt and is denoted as $F_k = F(k\Delta t)$ according to the discretization. The conditional probability p that F_{j+1} takes the same value

as F_j is given by

$$p = e^{-\Delta t/\tau_f}, \quad (32)$$

and the probability q that F_{k+1} is different from F_k is therefore obtained as

$$q = 1 - p. \quad (33)$$

The probabilistic model is then defined as follows:

- We introduce the variable s_k at a discretized time $k\Delta t$ which takes two values ± 1 .
- s_k and F_k are initially set to $s_0 = +1$ and $F_0 = +H_0$, respectively.
- s_k jumps from $+1$ (-1) to -1 ($+1$) only if F_k continues to take the identical value $-H_0$ ($+H_0$) for a time interval longer than $n_{ch}\Delta t$.
- s_k does not jump from $+1$ (-1) to -1 ($+1$) even though F_k continues to take $+H_0$ ($-H_0$) for any time interval longer than $n_{ch}\Delta t$.

A. Average time $\bar{\tau}$ of the passage time through the channel

We first derive the exact expression for the average time $\bar{\tau}$ passing through the channel in terms of the probabilistic model. In considering a time series of F_k , $\bar{\tau}$ is evaluated as

$$\bar{\tau} = \sum_l l\Delta t \sum_{0 \leq k \leq l} g_{k,l}^{(n_{ch})} q^k p^{l-k} \Big|_{q=1-p}. \quad (34)$$

Here $g_{k,l}^{(n_{ch})}$ is the number of the time sequences $\{F_j\}$ for $0 \leq j < l$ where the value of F_j is changed k times in each $\{F_j\}$ and s_j jumps from $+1$ to -1 for the first time at $t = l\Delta t$.

Equation (34) is, furthermore, reexpressed as

$$\bar{\tau} = \hat{T}Q_{n_{ch}}(q, p) \Big|_{q=1-p}, \quad (35)$$

where \hat{T} is the differential operator defined by

$$\hat{T} \equiv \Delta t \left(q \frac{\partial}{\partial q} + p \frac{\partial}{\partial p} \right), \quad (36)$$

and $Q_{n_{ch}}(q, p)$ is the quantity defined by

$$Q_{n_{ch}}(q, p) \equiv \sum_l \sum_{0 \leq k \leq l} g_{k,l}^{(n_{ch})} q^k p^{l-k}. \quad (37)$$

One should note that the q - and p -dependences in $Q_{n_{ch}}$ are crucial and that q and p are considered to be independent in Eq. (37).

The explicit form of $Q_{n_{ch}}(q, p)$ is then determined to satisfy the following conditions:

- In considering any length of time series of F_k , there exists a time interval of length n_{ch} in the last of the time series, where all the F_k take the same value $-H_0$, i.e., the condition that s_k jumps from $+1$ to -1 is satisfied.
- The condition for s_k to jump from $+1$ to -1 is not satisfied before the last time interval.

One should note that the equality $Q_n(1-p, p) = 1$ holds for any n , because the time interval described above always exists somewhere in a long time series. Particularly, for $n = n_{ch}$, $Q_{n_{ch}}(1-p, p)$ is obviously equal to the probability that s_j changes its sign which must be unity for $H_0 > H_c$.

The explicit form of $Q_n(q, p)$, as shown in Appendix A, is given by

$$Q_n(q, p) = \frac{(1-p)qp^{n-1}}{(1-p)^2 - q^2(1-p^{n-1})}, \quad (38)$$

where $Q_n(1-p, p) = 1$ is certainly satisfied. Applying the operator (36) to the explicit form (38) with $n = n_{ch}$ yields the equation

$$\begin{aligned} \bar{\tau} &= \hat{T}Q_{n_{ch}}(q, p) \Big|_{q=1-p} = \Delta t \frac{2 - p^{n_{ch}-1}}{(1-p)p^{n_{ch}-1}} \\ &= \Delta t \frac{2 - e^{\Delta t/\tau_f} e^{-\tau_{ch}/\tau_f}}{(1 - e^{-\Delta t/\tau_f}) e^{\Delta t/\tau_f} e^{-\tau_{ch}/\tau_f}}, \end{aligned} \quad (39)$$

where the last equality is obtained by using Eqs. (32) and (33) with the relation $\tau_{ch} = n_{ch}\Delta t$.

The exact expression of $\bar{\tau}$ is finally given by

$$\bar{\tau} = \tau_f (2e^{\tau_{ch}/\tau_f} - 1) \quad (40)$$

in the limit of $\Delta t \rightarrow 0$ by keeping τ_{ch} constant. Equation (40) qualitatively agrees for $\tau_{ch}/\tau_f \gg 1$ with the result (31) determined by studying the correlation time τ_f of $F(t)$ and $p(\tau)$ which is the probability for $F(t)$ to continue to take a same value longer than time interval τ .

B. Distribution function $P(\tau)$ of the passage time τ through the channel

The distribution function $P(\tau)$ of the passage time τ through the channel s_{ch} is determined by solving the equation

$$P(\tau) = \delta(\tau - \hat{T})Q_{n_{ch}}(q, p) \Big|_{q=1-p}, \quad (41)$$

where $\delta(x)$ is the delta function. The Laplace transform $\mathcal{L}[P](z)$ should be calculated so as to solve Eq. (41). In using the expanded form of $Q_{n_{ch}}(q, p)$ given by Eq. (37), the Laplace transform is expressed as

$$\begin{aligned} \mathcal{L}[P](z) &\equiv \int_0^\infty e^{-\tau z} P(\tau) d\tau = e^{-z\hat{T}} Q_{n_{ch}}(q, p) \Big|_{q=1-p} \\ &= \sum_l \sum_{0 \leq k \leq l} g_{k,l}^{(n_{ch})} (e^{-z\Delta t} q)^k (e^{-z\Delta t} p)^{l-k} \Big|_{q=1-p}. \end{aligned} \quad (42)$$

Equation (42) reveals that $\mathcal{L}[P](z)$ can be obtained by replacing q and p by $e^{-z\Delta t}q$ and $e^{-z\Delta t}p$ in $Q_{n_{ch}}(q, p)$, respectively, i.e.,

$$\mathcal{L}[P(\tau)](z) = Q_{n_{ch}}(e^{-z\Delta t}q, e^{-z\Delta t}p) \Big|_{q=1-p}. \quad (43)$$

Substituting the explicit form (38) for $n = n_{ch}$ into Eq. (43) yields the equation

$$\mathcal{L}[P(\tau)](z) = \frac{(\tau_f z + 1)e^{-(z+\tau_f^{-1})\tau_{ch}}}{\tau_f^2 z^2 + 2\tau_f z + e^{-(z+\tau_f^{-1})\tau_{ch}}} \quad (44)$$

in the limit of $\Delta t \rightarrow 0$ by keeping τ_{ch} constant. By applying the inverse Laplace transform to Eq. (44), the distribution function $P(\tau)$ is analytically evaluated in the expanded form as

$$\begin{aligned} P(\tau) &= \tau_f^{-1} e^{-\tau/\tau_f} \sum_{k=0}^{\infty} \theta(t_{k+1}) \frac{(-x)^k}{k!} \frac{d^k}{dx^k} \cosh \sqrt{x} \Big|_{x=(t_{k+1})^2} \\ &= \tau_f^{-1} e^{-\tau/\tau_f} \left[\theta(t_1) \cosh(t_1) - \theta(t_2) \frac{t_2 \sinh(t_2)}{2} + \theta(t_3) \frac{t_3^2 \cosh(t_3) - t_3 \sinh(t_3)}{8} \right. \\ &\quad \left. - \theta(t_4) \frac{t_4^3 \sinh(t_4) - 3t_4^2 \cosh(t_4) + 3t_4 \sinh(t_4)}{48} + \dots \right], \end{aligned} \quad (45)$$

where $t_k(\tau) \equiv (\tau - k\tau_{ch})/\tau_f$ and $\theta(t)$ is the Heaviside function defined by

$$\theta(t) = \begin{cases} 1 & \text{for } t \geq 0 \\ 0 & \text{for } t < 0 \end{cases}. \quad (46)$$

For details of the derivation of Eq. (45), see Appendix B.

Let us suppose to truncate the expansion (45) at $k = k_c$. It should be noted that Eq. (45) gives the exact distribution for $0 < \tau < k_c \tau_{ch}$ even though the truncation is executed, since all the terms individually include $\theta(t_k)$ and so the terms for $k > k_c$ do not contribute to $P(\tau)$ for $\tau < k_c \tau_{ch}$. Equation (45) is compared with the numerically evaluated distribution in Fig. 14. One observes that the probabilistic model quantitatively explains the statistical property of passing through the channels. Namely, the figure exhibits that

- there exists a region where $P(\tau) = 0$ for $\tau < \tau_{ch}$, which presents the minimal time of passing through the channels,
- $P(\tau)$ decreases exponentially for $\tau \gg \tau_{ch}$, $P(\tau) \propto e^{-\alpha\tau}$ with a constant α ,
- the rate α increases as τ_f is increased. This tendency is consistent with the fact that the probability of passing through channels increases as τ_f is increased since the DSEF will often continue to take an identical value longer than τ_{ch} .

On the other hand, the expansion (45) starts to disagree with the correct value in an exponential way for $\tau > k_c \tau_{ch}$. Let us try to obtain the asymptotic solution of $P(\tau)$ for $\tau \gg \tau_{ch}$. Equation (B2) is approximated as

$$\langle e^{-z(\tau-\tau_{ch})} \rangle \simeq \frac{1}{1 + (\bar{\tau} - \tau_{ch})z} \quad \text{for } |z| \ll \tau_{ch}^{-1}, \quad (47)$$

where $\bar{\tau}$ is the average time of passing through the channel given in Eq. (40). The inverse Laplace transform of Eq. (47) is straightforwardly calculated to give

$$P(\tau) \simeq \frac{1}{\bar{\tau} - \tau_{ch}} \exp\left(-\frac{\tau - \tau_{ch}}{\bar{\tau} - \tau_{ch}}\right), \quad (48)$$

which reveals that $P(\tau)$ decreases exponentially with the damping rate $\alpha = (\bar{\tau} - \tau_{ch})^{-1}$ for $\tau \gg \tau_{ch}$.

C. Fourier spectrum $I(\omega)$ of a time series denoted by the probabilistic model

We derive the Fourier spectrum of the probabilistic model to focus on the dynamical characteristics in the SRM phase. The Fourier spectrum $I(\omega)$ is defined by

$$I(\omega) = \lim_{T \rightarrow \infty} \frac{1}{T} \left\langle \left| \int_0^T x(t) e^{-i\omega t} dt \right|^2 \right\rangle, \quad (49)$$

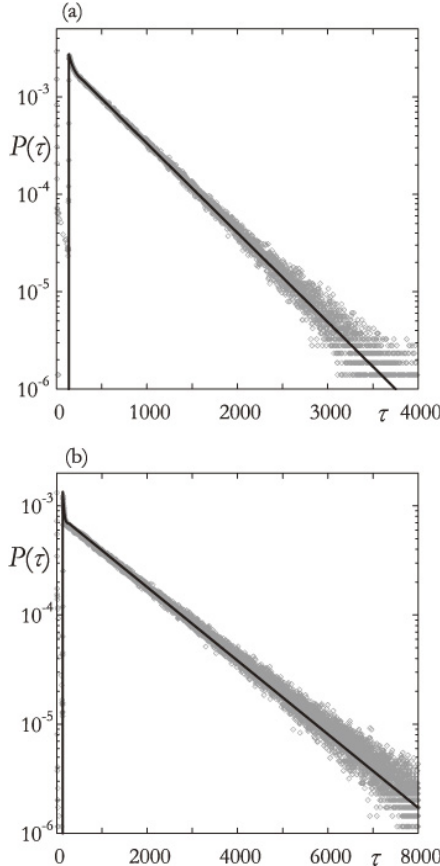


FIG. 14: Distribution functions $P(\tau)$ of time passing through channels. The theoretical results (solid lines) are compared with the numerically evaluated distributions (symbols) ($H_0 = 0.3852$) for (a) $\tau_f = 130$ and (b) $\tau_f = 50$. The external field is set to be $H_0 = 0.3852$ in both of the numerical simulations. τ_{ch} corresponding to the value of the external field is estimated to be $\tau_{ch} \simeq 134$ via the condition $P(\tau) \simeq 0$ for $\tau < \tau_{ch}$, where both (a) and (b) give the identical value of τ_{ch} . The expansion in Eq. (45) is summed over for $k \leq 60$, i.e., $k_c = 60$. The result assures that the probabilistic model is quite useful to explain the distribution of time passing through channels.

i.e., the ensemble average of the Fourier transform of the time series $x(t)$. Let us generate a time series $x_0(t)$ according to the sign of $s(t)$ such that $x_0(t) = +1$ if $s(t) > 0$ and $x_0(t) = -1$ otherwise. Then the time series is expressed as

$$x_0(t) = (-1)^{n-1}, \quad \text{for } t_{n-1} \leq t < t_n \quad (50)$$

with $n \geq 1$, where t_n denotes the n th time to cross zero for $s(t)$. Hereafter, t_0 is set to be zero without loss of generality. By identifying that $\tau_n \equiv t_n - t_{n-1}$ is independently distributed according to Eq. (45), one can obtain the Fourier spectrum of $x_0(t)$ by the probabilistic

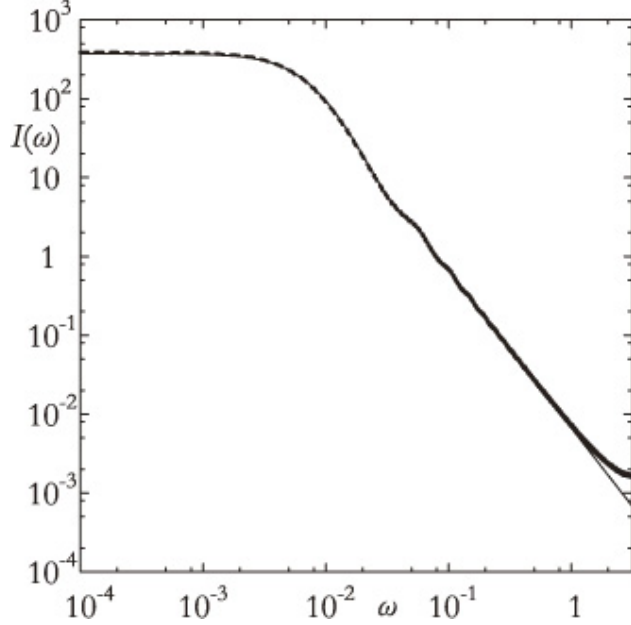


FIG. 15: Fourier spectrum obtained theoretically (line) and numerically (dashed line). $\tau_f = 130$ is set for both numerical and theoretical results, and the external field is set to be $H_0 = 0.3852$ in the numerical simulation. $\tau_{ch} = 134$ is used for Eq. (52) which is estimated in Fig. 14. The numerically evaluated time series $s(t)$ is normalized such that +1 if $s(t) > 0$ and -1 otherwise $s(t) < 0$ to generate $x_0(t)$ and its Fourier spectrum.

model as shown in Appendix C, in the form

$$I_0(\omega) = \frac{4}{\bar{\tau}\omega^2} \Re \left(\frac{1 - \langle e^{-i\omega\tau_n} \rangle}{1 + \langle e^{-i\omega\tau_n} \rangle} \right) = \frac{4}{\bar{\tau}\omega^2} \frac{1 - |\langle e^{-i\omega\tau_n} \rangle|^2}{|1 + \langle e^{-i\omega\tau_n} \rangle|^2} \quad (51)$$

where $\Re(X)$ represents the real part of X , and $\lim_{N \rightarrow \infty} \frac{t_N}{N} = \langle \tau_n \rangle = \bar{\tau}$ is used.

Substituting the explicit form of $\langle e^{-i\omega\tau_n} \rangle$ given in Eq. (44) with $z = i\omega$ into Eq. (51) eventually yields

$$I_0(\omega) = \left(\frac{4\tau_f}{\bar{\tau}\omega} \right) \frac{\omega^3\tau_f^3 + (4 - e^{-2\tau_{ch}/\tau_f})\omega\tau_f - 2e^{-\tau_{ch}/\tau_f}(\omega\tau_f \cos \omega\tau_{ch} + 2 \sin \omega\tau_{ch})}{(4 + \omega^2\tau_f^2)(\omega^2\tau_f^2 - 2\omega\tau_f e^{-\tau_{ch}/\tau_f} \sin \omega\tau_{ch} + e^{-2\tau_{ch}/\tau_f})}. \quad (52)$$

Equation (52) is confirmed by comparing with the numerically evaluated Fourier spectrum for the normalized time series $x_0(t)$ in Fig. 15.

Let us finally introduce a modified probabilistic model which is compatible with the numerically evaluated spectrum of the original time series $s(t)$ without normalization. Instead of Eq. (50), let us define

$$x(t) = (-1)^{n-1} [1 - a(t - t_{n-1})] \quad \text{for } t_{n-1} \leq t < t_n \quad (53)$$

with $n \geq 1$, where $a(\Delta t)$ incorporates the wave form of the time series passing through the channel and is assumed to be $a(\Delta t) = 0$ for $\Delta t > \tau_{ch}$. Note that by setting $a(\Delta t) = 0$ also for $\Delta t \leq \tau_{ch}$ the original probabilistic model is recovered. As shown in appendix C, the Fourier spectrum $I(\omega)$ for $x(t)$ as a modification to $I_0(\omega)$ is obtained in the form

$$I(\omega) = I_0(\omega) \frac{1 + |\hat{a}(\omega)|^2 + 2\Re[\hat{a}(\omega)]}{4}, \quad (54)$$

where

$$\hat{a}(\omega) \equiv 1 - i\omega \int_0^{\tau_{ch}} a(t) e^{-i\omega t} dt. \quad (55)$$

By approximating as $a(\Delta t) = 1 + |s_{ch}|$ for $0 < \Delta t < \tau_{ch}$, Eq. (54) reduces to

$$I(\omega) = I_0(\omega) \left(\frac{1 + s_{ch}^2}{2} + \frac{1 - s_{ch}^2}{2} \cos \omega \tau_{ch} \right). \quad (56)$$

Equation (56) is confirmed by comparing with the numerically evaluated Fourier spectrum in Fig. 16.

VII. CONCLUDING REMARKS

In this paper, we considered the time-dependent Ginzburg-Landau equation (3) under the dichotomous stochastic external field (DSEF) $F(t)$ with a finite correlation time in order to investigate the dynamics of the magnetization $s(t)$ of the ferromagnet system driven by the magnetic field of which the strength H_0 is constant and the direction is stochastically changed to its opposite.

It was found that the dynamics of $s(t)$ show two kinds of motion, i.e., the symmetry-restoring motion (SRM) and the symmetry-breaking motion (SBM), which are respectively observed when H_0 is larger or smaller than the critical value H_c . The transition line between SRM and SBM was analytically determined only by the external field strength and is independent of the correlation time τ_f of the applied field. These two distribution functions further imply that the ensemble average of $s(t)$ discontinuously changes at $H_0 = H_c$. These results are quite different from the system driven by a periodically oscillating field [12].

We then discussed the average time $\bar{\tau}$ of passing through the channels slightly above H_c and found that it depends on $H_0 - H_c$ and τ_f as

$$\bar{\tau} \simeq \tau_f \exp \left[\frac{C}{\tau_f (H_0 - H_c)^{1/2}} \right], \quad (57)$$

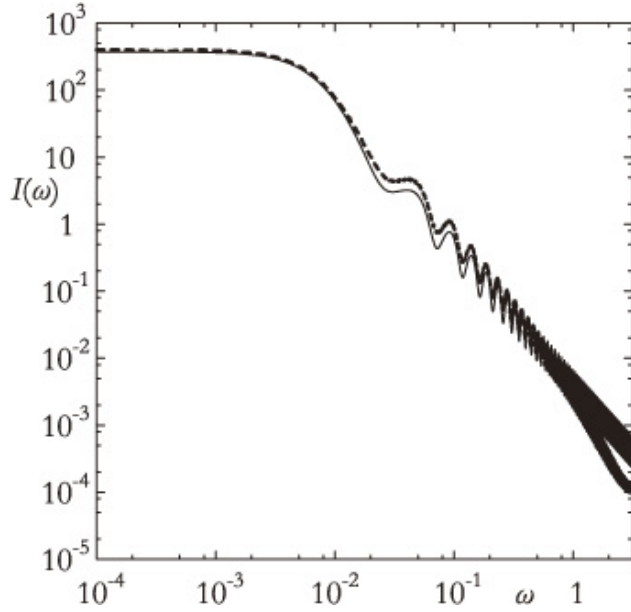


FIG. 16: Theoretically obtained Fourier spectrum (56) drawn by the solid line is compared with the numerical result drawn by the dashed line. $\tau_f = 130$ is set for both numerical and theoretical result, and the external field is set to be $H_0 = 0.3852$ in the numerical simulation. $\tau_{ch} = 134$ is used for Eq. (52) which is estimated in Fig. 14. Here the Fourier transform is directly applied to the numerically evaluated time series $s(t)$ without normalization and the Fourier spectrum is compared with Eq. (56) for $s_{ch} = 1/\sqrt{3}$.

which has a form similar to that of the average duration between neighboring phase slips of the phase difference in the phase synchronization observed in coupled chaotic systems [19, 20, 21, 22, 23, 24, 25].

Furthermore, a probabilistic model proposed to simplify the dynamics of passing through a channel for $H_0 > H_c$ was investigated to analytically discuss the statistical characteristics of the process. By obtaining the probability $Q_n(q, p)$ of $s(t)$ passing through a channel, the average time $\bar{\tau}$ of passing through the channel, the distribution function $P(\tau)$ of the passage time τ and the Fourier spectrum $I(\omega)$ of the time series denoted by the probabilistic model were evaluated in an analytical way. The statistics obtained by the probabilistic model were in quantitative agreement with the numerically obtained results.

In closing the paper, it is worth noting that the application of the dichotomous noise field is quite different from that of Gaussian noise and produces a new dynamical response of the systems. It is quite interesting to examine the statistical characteristics obtained in

this paper in laboratory experiments, and also in other numerical simulations, e.g., Monte Carlo simulations.

VIII. ACKNOWLEDGMENTS

The authors wish to thank N. Tsukamoto, N. Fujiwara, and H. Hata for valuable comments. This study was partially supported by Grant-in-Aid for Scientific Research (C) of the Ministry of Education, Culture, Sports, Science, and Technology, and the 21st Century COE Program “Center Of Excellence for Research and Education on Complex Functional Mechanical Systems” at Kyoto University.

APPENDIX A: EXPLICIT FORM OF $Q_n(q, p)$

First of all, notice that each sample path of F_k ($k = 0, 1, 2, \dots$) corresponds to a symbol sequence of $\{+, -\}$. Let w be a symbol sequence of $\{+, -\}$, which is referred to as a string, and, for given sets A and B of strings, let AB be the set of all strings expressed as ab for $a \in A$ and $b \in B$, where ab denotes the concatenated string of a followed by b . In the following, the set composed of only one string w will be simply expressed as w . Further, let $(A)_n$ be the set of all strings expressed as

$$a_1 a_2 \cdots a_k \quad (\text{A1})$$

with $a_i \in A$ and $0 \leq k \leq n$, where $k = 0$ means the zero length string, including the case $a_i = a_j$ for $i \neq j$. Then, with this notation, every possible sequence starting with $+$ and terminating with successive $-$'s of length n ($n \geq 2$), which firstly appears in that string, can be summarized as

$$S_n \equiv (+(+)_\infty - (-)_{n-2})_\infty + (+)_\infty \overbrace{--\cdots-}^{n \text{ symbols}}. \quad (\text{A2})$$

For a given set S of strings, let us define its “probability” as a function of p and q by

$$P(q, p; S) \equiv \sum_{w \in S} P_w(p, q) \equiv \sum_{w \in S} p^{k(w)} q^{l(w)}, \quad (\text{A3})$$

where $P_w(p, q)$ denotes the probability for a string w , and $k(w)$ and $l(w)$ denote the numbers of pairs of identical symbols $(--, ++)$ and different symbols $(-+, +-)$ appearing in w ,

respectively. For given strings w_1 and w_2 , obviously, the identity

$$P_{w_1 w_2}(q, p) = P_{w_1 \sigma}(q, p) P_{w_2}(q, p) \quad (\text{A4})$$

holds with σ being the first symbol in w_2 , and we call $w_1 \sigma$ and w_2 a decomposition of the string $w \equiv w_1 w_2$. By noting that

$$Q_n(q, p) = P(q, p; S_n) \quad (\text{A5})$$

and considering decompositions of each element in S_n , $Q_n(q, p)$ can be expressed as

$$Q_n(q, p) = P(q, p; S'_n) P(q, p; R) p^{n-1}, \quad (\text{A6})$$

where

$$S'_n \equiv (+(+)_\infty - (-)_{n-2})_\infty + \quad (\text{A7})$$

and

$$R \equiv +(+)_\infty - . \quad (\text{A8})$$

Since each element of S'_n can be uniquely decomposed into a multiple of elements in

$$S''_n \equiv +(+)_\infty - (-)_{n-2} + \quad (\text{A9})$$

and inversely every multiple of elements in S''_n uniquely corresponds to an element in S'_n as its decomposition,

$$P(q, p; S'_n) = \sum_{j=0}^{\infty} [P(q, p; S''_n)]^j \quad (\text{A10})$$

$$= \frac{1}{1 - P(q, p; S''_n)} \quad (\text{A11})$$

is obtained. Finally, $P(q, p; R)$ and $P(q, p; S''_n)$ are calculated as

$$P(q, p; R) = q \sum_{j=0}^{\infty} p^j = \frac{q}{1 - p} \quad (\text{A12})$$

and

$$P(q, p; S''_n) = \sum_{j=0}^{\infty} p^j q \sum_{i=0}^{n-2} p^i q = q^2 \frac{1 - p^{n-1}}{(1 - p)^2}, \quad (\text{A13})$$

which yield Eq. (38) together with (A6) and (A11).

APPENDIX B: DERIVATION OF THE PROBABILITY DISTRIBUTION FUNCTION $P(\tau)$

Let us evaluate the inverse Laplace transform of Eq. (44) in order to derive the explicit form of $P(\tau)$. For simplicity, let us rescale the time so as to be $\tau_f = 1$. Then Eq. (44) is rewritten as

$$\langle e^{-z\tau} \rangle = \frac{(1+z)e^{-(1+z)\tau_{ch}}}{(1+z)^2 - (1 - e^{-(1+z)\tau_{ch}})}, \quad (B1)$$

which reads

$$\mathcal{L}[P(\tau + \tau_{ch})] = \langle e^{-z(\tau - \tau_{ch})} \rangle = \frac{e^{-\tau_{ch}}}{1+z - \frac{1-e^{-(1+z)\tau_{ch}}}{1+z}} = e^{-\tau_{ch}} \sum_{n=0}^{\infty} \frac{(1-e^{-(1+z)\tau_{ch}})^n}{(1+z)^{2n+1}}. \quad (B2)$$

By repeatedly applying the formula

$$\mathcal{L}^{-1} \left[e^{-(1+z)\tau_{ch}} \hat{f}(z) \right] = e^{-\tau_{ch}} f(\tau - \tau_{ch}) = e^{-\tau_{ch}} e^{-\tau_{ch} \frac{d}{d\tau}} f(\tau) = e^{-\tau_{ch}} e^{-\tau_{ch} \frac{d}{d\tau}} \mathcal{L}^{-1}[\hat{f}(z)] \quad (B3)$$

with $f(\tau) \equiv \mathcal{L}^{-1}[\hat{f}(z)]$, one obtains

$$\begin{aligned} \mathcal{L}^{-1} \left[\frac{(1-e^{-(1+z)\tau_{ch}})^n}{(1+z)^{2n+1}} \right] &= (1-e^{-\tau_{ch}} e^{-\tau_{ch} \frac{d}{d\tau}})^n \mathcal{L}^{-1} \left[\frac{1}{(1+z)^{2n+1}} \right] \\ &= (1-e^{-\tau_{ch}} e^{-\tau_{ch} \frac{d}{d\tau}})^n \frac{\tau^{2n}}{(2n)!} e^{-\tau} \theta(\tau), \end{aligned} \quad (B4)$$

where $\theta(\tau)$ denotes the Heaviside function Eq. (46), and the formula

$$\mathcal{L}^{-1} \left[\frac{1}{(1+z)^m} \right] = \frac{\tau^{m-1}}{(m-1)!} e^{-\tau} \theta(\tau) \quad (B5)$$

for any positive integer m is used. Thus, the inverse Laplace transform of Eq. (B2) reads

$$\begin{aligned} P(\tau + \tau_{ch}) &= e^{-\tau_{ch}} \sum_{n=0}^{\infty} \left(1 - e^{-\tau_{ch}} e^{-\tau_{ch} \frac{d}{d\tau}} \right)^n \frac{\tau^{2n}}{(2n)!} e^{-\tau} \theta(\tau) \\ &= e^{-(\tau + \tau_{ch})} \sum_{n=0}^{\infty} \left(1 - e^{-\tau_{ch} \frac{d}{d\tau}} \right)^n \frac{\tau^{2n}}{(2n)!} \theta(\tau), \end{aligned} \quad (B6)$$

where the identity

$$e^{-\tau_{ch}} e^{-\tau_{ch} \frac{d}{d\tau}} e^{-\tau} = e^{-\tau} e^{-\tau_{ch} \frac{d}{d\tau}} \quad (B7)$$

is used. By denoting the identity

$$\left(1 - e^{-\tau_{ch} \frac{d}{d\tau}}\right)^n = \sum_{k=0}^n \frac{(-e^{-\tau_{ch} \frac{d}{d\tau}})^k}{k!} \frac{d^k x^n}{dx^k} \Big|_{x=1} = \sum_{k=0}^{\infty} \frac{e^{-k\tau_{ch} \frac{d}{d\tau}} (-1)^k}{k!} \left(\frac{d}{dx}\right)^k x^n \Big|_{x=1} \quad (\text{B8})$$

Eq. (B6) is further simplified as

$$\begin{aligned} P(\tau + \tau_{ch}) &= e^{-(\tau + \tau_{ch})} \sum_{n=0}^{\infty} \sum_{k=0}^{\infty} e^{-k\tau_{ch} \frac{d}{d\tau}} \frac{(-1)^k}{k!} \left(\frac{d}{dx}\right)^k x^n \frac{\tau^{2n}}{(2n)!} \theta(\tau) \Big|_{x=1} \\ &= e^{-(\tau + \tau_{ch})} \sum_{k=0}^{\infty} e^{-k\tau_{ch} \frac{d}{d\tau}} \frac{(-1)^k}{k!} \left(\frac{d}{dx}\right)^k \cosh(\sqrt{x}\tau) \theta(\tau) \Big|_{x=1} \\ &= e^{-(\tau + \tau_{ch})} \sum_{k=0}^{\infty} e^{-k\tau_{ch} \frac{d}{d\tau}} \theta(\tau) \frac{(-\tau^2)^k}{k!} \left(\frac{d}{dx}\right)^k \cosh \sqrt{x} \Big|_{x=\tau^2} \\ &= e^{-(\tau + \tau_{ch})} \sum_{k=0}^{\infty} \theta(t_k) \frac{(-x)^k}{k!} \frac{d^k}{dx^k} \cosh \sqrt{x} \Big|_{x=t_k^2}, \end{aligned} \quad (\text{B9})$$

where $t_k(\tau) \equiv \tau - k\tau_{ch}$ and $\sum_{n=0}^{\infty} \frac{x^n}{(2n)!} = \cosh \sqrt{x}$ is used. After the replacement $\tau \rightarrow \tau - \tau_{ch}$, the rescaling of time as $\tau \rightarrow \tau/\tau_f$ and $\tau_{ch} \rightarrow \tau_{ch}/\tau_f$ in order to recover τ_f finally leads Eq. (B9) to Eq. (45).

APPENDIX C: DERIVATION OF THE FOURIER SPECTRUM $I(\omega)$

In this appendix, we formulate the Fourier spectrum of the time series of the magnetization $x(t)$ for the probabilistic model. Let $\tau_1, \tau_2, \tau_3, \dots$ be a sequence of mutually independent random variables having the probability density $P(\tau)$ obeying the condition $P(\tau) = 0$ for $\tau < \tau_{ch}$, i.e., $\tau_k \geq \tau_{ch}$. We introduce

$$x(t) = (-1)^n [1 - a(t - t_{n-1})] \text{ for } t_{n-1} \leq t < t_n, \quad (\text{C1})$$

where $t_n \equiv \sum_{k=1}^N \tau_k$ and $a(\Delta t)$ is a function satisfying $a(\Delta t) = 0$ for $\Delta t > \tau_{ch}$. We assume that the time series of the magnetization is approximately expressed by $x(t)$ with an appropriate form of $a(t)$. The Fourier transform of $x(t)$ follows

$$\begin{aligned} \int_0^{t_N} x(t) e^{-i\omega t} dt &= \sum_{n=1}^N (-1)^{n-1} \int_{t_{n-1}}^{t_n} [1 - a(t - t_{n-1})] e^{-i\omega t} dt \\ &= \sum_{n=1}^N (-1)^{n-1} e^{-i\omega t_{n-1}} \left[\int_0^{\tau_n} e^{-i\omega t} dt - \int_0^{\tau_{ch}} a(t) e^{-i\omega t} dt \right] \\ &= \sum_{n=1}^N (-1)^n e^{-i\omega t_{n-1}} \frac{e^{-i\omega \tau_n} - \hat{a}(\omega)}{i\omega}, \end{aligned} \quad (\text{C2})$$

where

$$\hat{a}(\omega) \equiv 1 - i\omega \int_0^{\tau_{ch}} a(t) e^{-i\omega t} dt. \quad (C3)$$

By considering the absolute square of Eq. (C2) and then taking the ensemble average,

$$\begin{aligned} \omega^2 \left| \int_0^{t_N} x(t) e^{-i\omega t} dt \right|^2 &= \sum_{n=1}^N |e^{-i\omega\tau_n} - \hat{a}(\omega)|^2 \\ &+ 2\Re \left[\sum_{1 \leq m < n \leq N} (-1)^{n-m} e^{-i\omega \sum_{k=m+1}^{n-1} \tau_k} (e^{-i\omega\tau_n} - \hat{a}(\omega)) (1 - e^{-i\omega\tau_m} \hat{a}^*(\omega)) \right] \end{aligned} \quad (C4)$$

and

$$\begin{aligned} \frac{\omega^2}{N} \left\langle \left| \int_0^{t_N} x(t) e^{-i\omega t} dt \right|^2 \right\rangle &= 1 + |\hat{a}(\omega)|^2 - 2\Re [\langle e^{-i\omega\tau_n} \rangle \hat{a}^*(\omega)] \\ &+ 2N^{-1} \Re \left[\sum_{1 \leq m < n \leq N} (-1)^{n-m} \langle e^{-i\omega\tau_k} \rangle^{n-m-1} (\langle e^{-i\omega\tau_k} \rangle - \hat{a}(\omega)) (1 - \langle e^{-i\omega\tau_k} \rangle \hat{a}^*(\omega)) \right] \end{aligned} \quad (C5)$$

are obtained. Since $|\langle e^{-i\omega\tau_n} \rangle| < 1$, in the limit of $N \rightarrow \infty$, the last term in Eq. (C5) reads

$$\begin{aligned} &-2\Re \left[\sum_{k=0}^{\infty} (-1)^k \langle e^{-i\omega\tau_n} \rangle^k (\langle e^{-i\omega\tau_n} \rangle - \hat{a}(\omega)) (1 - \langle e^{-i\omega\tau_n} \rangle \hat{a}^*(\omega)) \right] \\ &= -2\Re \left[\frac{\langle e^{-i\omega\tau_n} \rangle (1 + |\hat{a}(\omega)|^2) - \hat{a}(\omega) - \langle e^{-i\omega\tau_n} \rangle^2 \hat{a}^*(\omega)}{1 + \langle e^{-i\omega\tau_n} \rangle} \right], \end{aligned} \quad (C6)$$

which leads to

$$\lim_{N \rightarrow \infty} \frac{1}{N} \left\langle \left| \int_0^{t_N} x(t) e^{-i\omega t} dt \right|^2 \right\rangle = \omega^{-2} \Re \left[\frac{1 - \langle e^{-i\omega\tau_n} \rangle}{1 + \langle e^{-i\omega\tau_n} \rangle} \right] (1 + |\hat{a}(\omega)|^2 + 2\Re[\hat{a}(\omega)]). \quad (C7)$$

By noting that $\lim_{N \rightarrow \infty} \frac{t_N}{N} = \langle \tau_n \rangle = \bar{\tau}$,

$$I(\omega) = I_0(\omega) \frac{1 + |\hat{a}(\omega)|^2 + 2\Re[\hat{a}(\omega)]}{4} \quad (C8)$$

is obtained, where

$$I_0(\omega) \equiv \frac{4}{\omega^2 \bar{\tau}} \Re \left[\frac{1 - \langle e^{-i\omega\tau_n} \rangle}{1 + \langle e^{-i\omega\tau_n} \rangle} \right] \quad (C9)$$

corresponds to the case that $a(\Delta t) = 0$ for all $\Delta t \geq 0$ and thus $x(t) = (-1)^n$ for $t_{n-1} \leq t < t_n$.

[1] T. Tomé, and M. J. de Oliveira, Phys. Rev. A **41**, 4251 (1990).

[2] J. F. F. Menders, and E. J. S. Large, J. Stat. Phys. **64**, 653 (1991).

[3] W. S. Lo and R. A. Pelcovits, Phys. Rev. A **42**, 7471 (1990)

[4] M. Acharyya, Phys. Rev. E **56**, 1234 (1997).

[5] M. Acharyya, Phys. Rev. E **56**, 2407 (1997); M. Acharyya, Phys. Rev. E **58**, 179 (1998); M. Acharyya, Phys. Rev. E **59**, 218 (1999);

[6] S. W. Sides, P. A. Rikvold, and M. A. Novotny, Phys. Rev. Lett. **81**, 834 (1998).

[7] S. W. Sides, P. A. Rikvold, and M. A. Novotny, Phys. Rev. E **59**, 2710 (1999).

[8] P. A. Rikvold *et al.*, in *Computer Simulation Studies in Condensed Matter Physics XIII*, edited by D. P. Landau, S. P. Lewis, and H.-B. Schüttler, (Springer, Berlin, 2000), pp. 105-119.

[9] G. Korniss, C. J. White, P. A. Rikvold, and M. A. Novotny, Phys. Rev. E **63**, 016120 (2001)

[10] Q. Jiang, H.-N. Yang, and G.-C. Wang, Phys. Rev. B **52**, 14911 (1995).

[11] Q. Jiang, H.-N. Yang, and G.-C. Wang, J. Appl. Phys. **79**, 5122 (1996).

[12] H. Fujisaka, H. Tutu, and P. A. Rikvold, Phys. Rev. E **63**, 036109 (2001).

[13] T. Yasui, H. Tutu, M. Yamamoto, and H. Fujisaka, Phys. Rev. E **66**, 036123 (2002).

[14] H. Tutu and N. Fujiwara, J. Phys. Soc. Japan, **73**, 2680 (2004).

[15] K. Kitahara, W. Horsthemke, and R. Lefever, Phys. Lett. **A70**, 377 (1979).

[16] W. Horsthemke and R. Lefever, Phys. Lett. **64A**, 19 (1977).

[17] K. Kitahara, W. Horsthemke, R. Lefever, and Y. Inaba, Prog. Theor. Phys. **64**, 4 (1980).

[18] W. Horsthemke and R. Lefever, in *Noise-Induced Transitions* (Springer, Berlin, 1984), in Sec. 9.

[19] M. G. Rosenblum, A. S. Pikovsky and J. Kurths, Phys. Rev. Lett. **76**, 1804 (1996).

[20] A. Pikovsky, G. Osipov, M. Rosenblum, M. Zaks, and J. Kurths, Phys. Rev. Lett. **79**, 47 (1997).

[21] S. Boccaletti, E. Allaria, R. Meucci, and F. T. Arecchi, Phys. Rev. Lett. **89**, 194101 (2002).

[22] E. Rosa, E. Ott, and M. H. Hess, Phys. Rev. Lett. **80**, 1642 (1998).

[23] K. J. Lee, Y. Kwak, and T. K. Lim, Phys. Rev. Lett. **81**, 321 (1998).

[24] H. Fujisaka, T. Yamada, G. Kinoshita, and T. Kono, Physica D **204**, (2005).

[25] H. Fujisaka, S. Uchiyama, and T. Horita, Prog. Theor. Phys. **114** (2005).